# THz Letters

## Subharmonic Injection Locking for Phase and Frequency Control of RTD-Based THz Oscillator

Khaled Arzi, Safumi Suzuki, Andreas Rennings, *Member, IEEE*, Daniel Erni, *Member, IEEE*, Nils Weimann, *Member, IEEE*, Masahiro Asada, *Fellow, IEEE*, and Werner Prost

***Abstract*—Phase and frequency control of resonant tunneling diode (RTD) based terahertz oscillators are major challenges in realizing coherent signal sources for arrayed applications, such as spatial power combining, beam steering, or multi-in multi-out systems. In this letter, we demonstrate frequency locking and control of an RTD oscillating at $f_0 \sim 550$ GHz, via radiative injection of a weak sinusoidal subharmonic signal at $f_0/2$. Precise frequency control, within the locking range of around 2 GHz, is demonstrated. A peak output power enhancement of 14 dB in the whole locking range, compared to the free running oscillator, is achieved. Furthermore, occurrence of phase locking is identified by the spectral linewidth reduction, quantifiable in the full-width at half-maximum parameter. A signal linewidth of 490 Hz was achieved in locked operation.**

***Index Terms*—Beam steering, injection-locked oscillators, phase control, resonant tunneling device, terahertz radiation.**

### I. Introduction

THERE is vital interest in compact and energy-efficient solid-state sources operating at room temperature to bridge the terahertz gap $(0.3\,\mathrm{THz} < f_{\mathrm{THz}} < 3\,\mathrm{THz})$, especially within mobile scenarios. Possible applications are manifold including ultrahigh-speed wireless communications, spectroscopy, radar, and imaging. Fundamental mode optical terahertz oscillators based on p-type Ge [1] or quantum cascade lasers [2], [3] offer high output power but require cryogenic operation, and are lacking power efficiency around 1 THz. Advanced, ultrascaled transistor devices based on InP [4], [5] and on silicon (Si) [6], [7] have recently become available for electronic terahertz circuits.

Fundamental mode sources up to 0.57 THz utilizing the InP HBT technology [8] and 1 THz harmonic oscillation by SiGe HBTs [9] have been demonstrated. Two-terminal devices with relaxed scaling rules, such as impact ionization avalanche transit time diodes, tunneling transit-time diodes, and Gunn diodes, are also intensively studied as they can offer oscillation frequencies in the sub-THz range [10]. A very promising candidate for terahertz sources is the resonant tunneling diode (RTD), which can be monolithically integrated into an on-chip antenna for orthogonal [11], [12] or in-plane [13] free-space emission. RTD-based oscillators operating at room temperature are currently providing the highest oscillation frequency of any solid-state electronic devices at around 2 THz [14]. As a fundamental oscillator, the RTD may be operated at higher power efficiency as compared to frequency multiplying devices.

Frequency and phase control of oscillators are major challenges at terahertz frequencies but indispensable in order to provide new array-based functionalities, such as spatial power combining, multi-in multi-out systems, or beam steering [15]–[17]. In addition, sharp spectral linewidth and tunability of the oscillation frequency at terahertz frequencies are required for the applications under consideration. Conventionally, the frequency control of RTD-based oscillators is carried out by integration of a voltage-controlled capacitance [18]. At the expense of an added capacitive load, this method provides a large frequency tuning range, but frequency and phase fluctuations of the free running oscillator are not reduced. A signal stabilization and even phase locking of a free running RTD oscillator are presented in [19] with an external phase-locked-loop circuit. However, many components such as heterodyne mixer, low-noise amplifier, balanced mixer, loop filter, and external signal generator are needed. High-$Q$ passive resonators may be used for frequency stabilization, but in general lack tunability. A less complex

Manuscript received April 23, 2019; revised July 23, 2019; accepted December 2, 2019. Date of publication January 27, 2020; date of current version March 3, 2020. This work was supported in part by the Deutsche Forschungsgemeinschaft within the Collaborative Research Center SFB/TRR 196 MARIE (Projects C02 and C05) and in part by the Scientific Grant-in-Aid from Japan Society for the Promotion of Science (16H06292). The work of S. Suzuki was supported by a Mercator Fellowship Grant. *(Corresponding author: Khaled Arzi.)*

K. Arzi, N. Weimann, and W. Prost are with the High Frequency Electronic Component Department (BHE), Faculty of Engineering, University of Duisburg-Essen, and the Center for Nanointegration Duisburg-Essen, Duisburg D-47048, Germany (e-mail: khaled.arzi@uni-due.de; nils.weimann@uni-due.de; werner.prost@uni-duisburg-essen.de).

S. Suzuki is with the Department of Electrical and Electronic Engineering, Tokyo Institute of Technology, Tokyo 152-8552, Japan (e-mail: suzuki.s.av@m.titech.ac.jp).

A. Rennings and D. Erni are with the Laboratory for General and Theoretical Electrical Engineering (ATE), Faculty of Engineering, University of Duisburg-Essen, and Center for Nanointegration Duisburg-Essen, Duisburg D-47048, Germany (e-mail: andre.rennings@uni-due.de; daniel.erni@uni-due.de).

M. Asada is with the Department of Electrical and Electronic Engineering and the Institute of Innovative Research, Tokyo Institute of Technology, Tokyo 152-8552, Japan (e-mail: asada@pe.titech.ac.jp).

Color versions of one or more of the figures in this article are available online at https://ieeexplore.ieee.org.

Digital Object Identifier 10.1109/TTHZ.2019.2959411

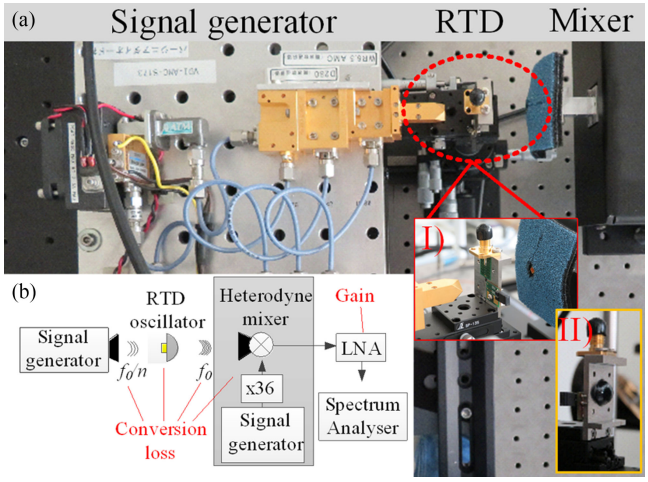


Fig. 1. (a) Measurement setup used to measure the locking range of a free running THz oscillator. (I) A closer look-up to the devices. (II) A front view of the RTD oscillator. (b) Schematic setup presentation showing the conversion losses occurring in the measurement path.

alternative that is even easily integrated into a mobile device is signal injection locking [20], [21]. This mechanism showed excellent results at microwave frequencies [16], [22], [23].

In this work, we provide proof of concept for the injection locking mechanism by radiative injection of a subharmonic signal into a sub-mm wave ($f_0 > 550\,\text{GHz}$) RTD-based fundamental mode oscillator.

## II. Devices and Measurement Setup

The fundamental mode oscillator consists of an RTD that is monolithically integrated with an on-chip slot antenna. A packaged RTD oscillator was used in this experiment. The RTD layer structure included thin barriers and wells in order to achieve high current density operation [24]. An offset-fed slot antenna was used for high-power operation [25]. The oscillator was placed on a hemispherical Si lens with 10 mm diameter collecting the output beam at the bottom side of the InP wafer. The RTD exhibits a maximum current density of 35 mA/$\mu$m$^2$ with a peak-to-valley current ratio of about 2. The oscillator starts oscillating when the RTD is biased in the regime of negative differential resistance (NDR). The frequency of oscillation is defined by the bias-dependent impedance of the RTD and the input impedance of the antenna. This device provides a free running oscillation frequency between 564 and 576 GHz, depending on the biasing point. The measurement setup for radiative injection and fundamental locking of the free running oscillator is shown in Fig. 1. The integrated RTD oscillator/antenna device used in this setup was designed for frequencies around $f_0 \sim 550\,\text{GHz}$ and was not yet optimized for efficient injection locking at the subharmonic injection signal $f_0/2$. The injection signal was generated with a frequency multiplying signal generator (AMC-370, VDI) connected to a WR3 horn antenna. The output power of the signal generator was measured using a power meter (PM5, VDI-Erickson). In the frequency range from 265 to 300 GHz, the variation of the output power $P_{\text{out}}$ was measured to 0–17 dBm and was considered for calibration. At the front side of the RTD oscillator, a heterodyne mixer (N9029AV, VDI) was placed, which exhibited a typical conversion loss of around 20 dB. A low-noise amplifier (BZR-P011800, B&Z) with a gain of 38 dB was introduced between the mixer and the spectrum analyzer in order to increase the measured power without degrading the phase noise. The loss path in the measurement setup can be deducted from Fig. 1(b). The Si lens introduced a 30% insertion loss in the transmitted beam. The effective area of the terahertz beam was calculated, including the Si lens area, to be 78.5 mm$^2$. The RTD's signal was collected at the mixer input through a horn antenna with gain of 26 dBi and calculated effective area of 8.8 mm$^2$. The mixer input was placed 12 mm away from the oscillator, resulting in a free-space path loss of 17 dB. The subsequent LNA introduced a signal gain of 38 dB.

## III. Measurements

The locking mechanism of the integrated RTD/antenna oscillator presented in this work was based on the following:

1) radiative injection, with a subharmonic signal frequency $f_{\text{inj}} \approx f_0/2$;
2) frequency multiplication by the RTD's nonlinearity, providing the locking signal;
3) transfer of the fundamental mode oscillation power to the locked signal power.

Under locked condition, the phase relation between master signal and fundamental mode oscillation is constant [20], [21]. The radiative injection mechanism decouples the locking master signal from the RTD oscillator, thus circumventing the lack of isolation inherent of two-terminal RTD devices.

To investigate the multiplication efficiency of the RTD, a signal at constant frequency of $f_{\text{inj}} = 293\,\text{GHz}$ was injected into the antenna. The power of the multiplied signal at $f_0 = 586\,\text{GHz}$ was recorded while varying the RTD's bias voltage within the NDR region. The NDR region of this device was between $V_{\text{RTD}} = 0.6\,\text{V}$ (peak point) and $V_{\text{RTD}} = 0.66\,\text{V}$ valley point. Due to the typical nonlinearity of the *I–V* curve in the NDR region, when the RTD was biased at the center of the NDR region ($V_{\text{RTD}} = 0.63\,\text{V}$), the power of the doubled frequency signal was at its minimum, i.e., the doubling efficiency exhibited a minimum. Biasing the RTD near the peak or valley point resulted in locked signals with higher RF power. Furthermore, the receiving efficiency of the RTD-slot devices at frequencies around $f_0/2$ is expected to be very low. This device is designed for only one resonant frequency $f_0$. Therefore, a high injection signal power ($\sim$20 mW) at $f_0/2$ needs to be radiated onto the device, resulting in a small signal injected into the RTD, which is then multiplied by the RTD's nonlinearity to the locking frequency $f_0$.

To investigate the locking range, a signal was injected at $f_{\text{inj}} \sim f_0/2$ (cf., Fig. 2). This frequency was increased stepwise [see Fig. 2(I)(a)–(c)] until frequency locking was observed [see Fig. 2(I)(c)]. The free running oscillator output power is $\sim$16 $\mu$W (measured with a power meter). The pulling of the

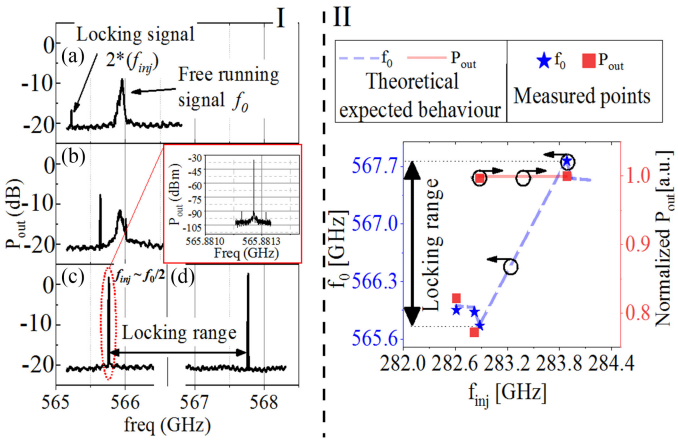


Fig. 2. Subharmonic injection and fundamental locking of a free running oscillator. The locking signal power is kept constant, and its oscillation frequency is increased stepwise until the RTD is locked, recorded with a resolution bandwidth of 1.3 MHz. The inset presents a close look-up (RBW = 100 Hz) of the locked signal spectrum. Fig. 2(II) shows the normalized power on the right *y*-axis and the oscillation frequency on the left *Y*-axis over the injected signal frequency.

RTD's oscillation frequency during synchronization is expected at frequency locking of a free running oscillator [26]. We observed a continuously increasing power transfer from the RTD's fundamental mode to the locked signal in Fig. 2(b) while the spectral width of the locked signal remains narrow. A locking range of 2 GHz was determined. Under the locked condition, the relatively wideband spectral power distribution of the initial RTD oscillator is compressed into the small bandwidth of the injected signal, resulting in a peak spectral power increase of about 14 dB (see Fig. 2(II) within locking range). Locking the free-running signal with a low-noise injection signal source narrows its linewidth [21]. The free-running signal is adopting the signal properties of the locking signal also in terms of signal purity. This behavior is experimentally verified and is presented in the inset of Fig. 2(I) (showing a close-up on the locked signal spectrum).

The spectral linewidth of the injection-locked oscillator is reduced to approximately the linewidth of the injected subharmonic signal, indicating phase locking. To quantify the locked signal purity, the peak's full-width at half-maximum (FWHM) is investigated. An FWHM value of the free running oscillator was measured to be 34.69 MHz (cf., Fig. 2(a), free running signal). After locking (cf., Fig. 2(c) and the inset), an FWHM value of 483 Hz was achieved. During the locking range, changing the frequency of the free running oscillator (by changing the bias point, within the locking range) does not alter the oscillation frequency. Conversely, this would lead to a relative phase change of the output signal, which can be exploited for the realization of beam steered RTD arrays. The locking range is defined as the frequency range between the start and end of the locking, and was found to be approximately proportional to $\sqrt{P_{\rm lock}/P_{\rm osc}}$, where $P_{\rm lock}$ is the locking signal and $P_{\rm osc}$ is the free running signal power.

## IV. Conclusion and Outlook

This work provides an experimental proof of radiative subharmonic injection and simultaneous frequency locking of a free running RTD-based oscillator at submillimeter wavelength. Compared to the free-running RTD oscillator, a significant increase in peak spectral signal power along with commensurate reduction of the spectral linewidth at 565 GHz was demonstrated. An FWHM value of around 34.69 MHz, when not locked, improved to less than 490 Hz, in locked operation. Achieving the locking condition requires a constant phase relation [20] between the master (subharmonic injection signal source) and the slave (the RTD-based oscillator); therefore, phase control of the RTD oscillator could be achieved. Further, circumventing the lack of isolation in the two-terminal RTD device, the radiative signal injection technique decouples the locking master signal from the RTD oscillator, thus enabling an architecture of phase-coupled RTD oscillator cores suitable for power-scalable integrated THz transmitter arrays.

## Acknowledgment

K. Arzi would like to thank CRC/TRR 196 MARIE for giving him the opportunity for a short-term scientific mission at the Tokyo Institute of Technology to perform the RF measurements.

## References

[1] S. Komiyama, "Far-infrared emission from population-inverted hot-carrier system in p-Ge," *Phys. Rev. Lett.*, vol. 48, pp. 271–274, 1982, doi: 10.1103/PhysRevLett.48.271.
[2] R. Köhler *et al.*, "Terahertz semiconductor heterostructure laser," *Nature*, vol. 417, pp. 156–159, 2002, doi: 10.1038/417156a.
[3] S. Fathololoumi *et al.*, "Terahertz quantum cascade lasers operating up to ∼ 200 K with optimized oscillator strength and improved injection tunneling," *Opt. Express*, vol. 20, pp. 3866–3876, 2012.
[4] M. Urteaga, Z. Griffith, M. Seo, J. Hacker, and M. J. W. Rodwell, "InP HBT technologies for THz integrated circuits," *Proc. IEEE*, vol. 105, no. 6, pp. 1051–1067, Jun. 2017.
[5] X. Mei *et al.*, "First demonstration of amplification at 1 THz using 25-nm InP high electron mobility transistor process," *IEEE Electron Device Lett.*, vol. 36, no. 4, pp. 327–329, Apr. 2015.
[6] A. Fox *et al.*, "Advanced heterojunction bipolar transistor for half-THz SiGe BiCMOS technology," *IEEE Electron Device Lett.*, vol. 36, no. 7, pp. 642–644, Jul. 2015.
[7] M. Schröter *et al.*, "SiGe HBT technology: Future trends and TCAD-based roadmap," *Proc. IEEE*, vol. 105, no. 6, pp. 1068–1086, Jun. 2017.
[8] M. Seo *et al.*, "InP HBT IC technology for terahertz frequencies: Fundamental oscillators up to 0.57 THz," *IEEE J. Solid-State Circuits*, vol. 46, no. 10, pp. 2203–2214, Oct. 2011.
[9] Z. Hu and R. Han, "Fully-scalable 2D THz radiating array: A 42-element source in 130-nm SiGe with 80-$\mu$W total radiated power at 1.01 THz," in *Proc. IEEE Radio Freq. Integr. Circuits Symp.*, 2017, pp. 372–375.
[10] H. Eisele, "480 GHz oscillator with an InP Gunn device," *Electron. Lett.*, vol. 46, no. 6, pp. 422–423, 2010, doi: 10.1049/el.2010.3362.
[11] S. Suzuki, M. Asada, A. Teranishi, H. Sugiyama, and H. Yokoyama, "Fundamental oscillation of resonant tunneling diodes above 1 THz at room temperature," *Appl. Phys. Lett.*, vol. 97, 2010, Art. no. 242102, doi: 10.1063/1.3525834.
[12] H. Kanaya, R. Sogabe, T. Maekawa, S. Suzuki, and M. Asada, "Fundamental oscillation up to 1.42 THz in resonant tunneling diodes by optimized collector spacer thickness," *J. Infrared, Millimeter, THz Waves*, vol. 35, no. 5, pp. 425–431, 2014, doi: 10.1007/s10762-014-0058-z.
[13] M. Feiginov, C. Sydlo, O. Cojocari, and P. Meissner, "Resonant-tunneling-diode oscillators operating at frequencies above 1.1 THz," *Appl. Phys. Lett.*, vol. 99, no. 23, 2011, Art. no. 233506, doi: 10.1063/1.3667191.

[14] R. Izumi, S. Suzuki, and M. Asada, "1.98 THz resonant-tunneling-diode oscillator with reduced conduction loss by thick antenna electrode," in *Proc. Int. Conf. Infrared, Millimeter, THz Waves*, Cancun, Mexico, Aug. 2017, Paper MA3.1.

[15] S.-H. Yan and T. H. Chu, "A beam-steering antenna array using injection locked coupled oscillators with self-tuning of oscillator free-running frequencies," *IEEE Trans. Antennas Propag.*, vol. 56, no. 9, pp. 2920–2928, Sep. 2008.

[16] R. A. York and T. Itoh, "Injection- and phase-locking techniques for beam control [antenna arrays]," *IEEE Trans. Microw. Theory Techn.*, vol. 46, no. 11, pp. 1920–1929, Nov. 1998.

[17] Y. Lo and J. Kiang, "Comparison of injection-locked and coupled oscillator arrays for beamforming," *IEEE Trans. Microw. Theory Techn.*, vol. 63, no. 4, pp. 1353–1360, Apr. 2015.

[18] S. Kitagawa, S. Suzuki, and M. Asada, "Wide frequency-tunable resonant tunnelling diode terahertz oscillators using varactor diodes," *Electron. Lett.*, vol. 52, no. 6, pp. 479–481, Mar. 17, 2016, doi: 10.1049/el.2015.3921.

[19] K. Ogino, S. Suzuki, and M. Asada, "Spectral narrowing of a varactor-integrated resonant-tunneling-diode terahertz oscillator by phase-locked loop," *J. Infrared, Millimeter, THz Waves*, vol. 38, pp. 1477–1486, 2017, doi: 10.1007/s10762-017-0439-1.

[20] R. Adler, "A study of locking phenomena in oscillators," *Proc. IEEE*, vol. 61, no. 10, pp. 1380–1385, Oct. 1973.

[21] B. Razavi, "A study of injection locking and pulling in oscillators," *IEEE J. Solid-State Circuits*, vol. 39, no. 9, pp. 1415–1424, Sep. 2004.

[22] S. Verghese, C. D. Parker, and E. R. Brown, "Phase noise of a resonant-tunneling relaxation oscillator," *Appl. Phys. Lett.* vol. 72, pp. 2550–2552, 1998, doi: 10.1063/1.121414.

[23] K. F. Tsang and C. M. Yuen, "Phase noise measurement of free-running microwave oscillators at 5.8 GHz using 1/3-subharmonic injection locking," *IEEE Microw. Wireless Compon. Lett.*, vol. 15, no. 4, pp. 217–219, Apr. 2005.

[24] H. Kanaya, T. Maekawa, S. Suzuki, and M. Asada, "Structure dependence of oscillation characteristics of resonant-tunneling-diode terahertz oscillators associated with intrinsic and extrinsic delay times," *Jpn. J. Appl. Phys.*, vol. 54, 2015, Art. no. 094103.

[25] S. Suzuki, M. Shiraishi, H. Shibayama, and M. Asada, "High-power operation of terahertz oscillators with resonant tunneling diodes using impedance-matched antennas and array configuration," *IEEE J. Sel. Topics Quantum Electron.*, vol. 19, no. 1, Feb. 2013, Art. no. 8500108.

[26] K. Arzi *et al.*, "Frequency locking of a free running resonant tunneling diode oscillator by wire-less sub-harmonic injection locking," in *Proc. 10th U.K.-Europe-China Workshop Millimetre Waves THz Technol.*, Liverpool, U.K., 2017, pp. 1–4, doi: 10.1109/UCMMT.2017.8068485.